THE JOURNAL OF BIOLOGICAL CHEMISTRY
Vol. 278, No. 27, Issue of July 4, pp. 24481–24490, 2003
Printed in U.S.A.

The Autoxidation of Tetrahydrobiopterin Revisited

PROOF OF SUPEROXIDE FORMATION FROM REACTION OF TETRAHYDROBIOPTERIN WITH MOLECULAR OXYGEN*

Received for publication, November 19, 2002, and in revised form, April 4, 2003
Published, JBC Papers in Press, April 24, 2003, DOI 10.1074/jbc.M211779200

Michael Kirsch‡§, Hans-Gert Korth¶, Verena Stenert¶, Reiner Sustmann¶, and Herbert de Groot‡

From the ‡Institut für Physiologische Chemie, Universitätsklinikum, Hufelandstrasse 55, D-45122 Essen and the ¶Institut für Organische Chemie, Universität Essen, Universitätsstr. 5, D-45117 Essen, Germany

It has been known for quite some time that tetrahydrobiopterin (H4B) is prone to autoxidation in the presence of molecular oxygen. Evidence has been presented that in this process superoxide radicals may be released, although their intermediacy never has been directly proven. In the present study, the autoxidation of H4B was reinvestigated with the aim to find direct evidence for superoxide formation. By means of two specific assays, namely elicitation of luminescence from lucigenin and ESR-spectrometric detection of the DEPMPO-OOH radical adduct, the release of free superoxide radicals was unequivocally demonstrated. The production of superoxide radicals was further corroborated by interaction with nitric oxide. The kinetics of the autoxidation process was established. Our data fully confirm earlier conclusions that the direct reaction between H4B and oxygen serves as an initiation reaction for the further, rapid reaction of the thus formed superoxide with H4B, thereby very likely establishing a chain reaction process involving reduction of molecular oxygen by the intermediary tetrahydrobiopterin radical. Conclusively, because H4B can *per se* induce oxidative stress, an *in vivo* overproduction of this pterin, as is evident in various diseases, may be responsible for the observed acceleration of pathophysiological pathways.

Tetrahydrobiopterin (H4B)[1] serves as an important cofactor for aromatic amino acid hydroxylases (1) as well as for all three NOS isoforms (2–5). At ambient temperature, H4B is not stable in the presence of molecular oxygen. In 1973, Fisher and Kaufman (6) noticed that the overall stoichiometry of the H_2O_2 yielding autoxidation of tetrahydrobiopterin, *i.e.* its spontaneous reaction with dioxygen, can in the presence of catalase be expressed as the following equation.

$$2\ H4B + O_2 \rightarrow 2\ H2B + 2\ H_2O \qquad \text{(Eq. 1)}$$

Fisher and Kaufman (6) additionally remarked that Cu,Zn-SOD inhibited autoxidation of H4B. One year later, Blair and Pearson (7, 8) analyzed the autoxidation of H4B in more detail. From the verification of the intermediacy of a tetrahydropterin radical cation, $H4B^{\cdot+}$ (at acidic pH), as well as from oxygen uptake experiments they speculated about the presence of a radical chain reaction mechanism in which the initiation step should proceed via electron transfer from H4B to oxygen, followed by rapid proton transfer (Equation 2).

$$H4B + O_2 \rightarrow [H4B^{\cdot+}, O_2^{\cdot-}] \rightarrow H3B^{\cdot} + HO_2^{\cdot} \qquad \text{(Eq. 2)}$$

$$H4B + HO_2^{\cdot} \rightarrow H3B^{\cdot} + H_2O_2 \qquad \text{(Eq. 3)}$$

$$H3B^{\cdot} + O_2 \rightarrow H2B + HO_2^{\cdot} \qquad \text{(Eq. 4)}$$

The following year, this mechanism was apparently proven by Nishikimi (9), who observed reduction of the $O_2^{\cdot-}$ scavenger nitro blue tetrazolium when the autoxidation of H4B was carried out at pH 7.4 in the presence of high amounts of Triton X-100. The conclusion of Nishikimi (9) was apparently supported by Heikkila and Cohen (10), who reported that reduction of ferricytochrome *c*, a common assay for superoxide, took place during autoxidation of H4B. However, it should be noted that tetrahydrobiopterin directly reduces cytochrome c^{3+}, with a rather high rate constant ($k = 3.4 \times 10^6\ M^{-1}\ s^{-1}$) (11, 12). Hence, H4B-dependent reduction of cytochrome c^{3+} cannot be used as evidence for the occurrence of reaction 2. Likewise, nitro blue tetrazolium reduction as applied by Nikishimi (9) can only be regarded as a weak indication for the intermediacy of superoxide, because Liochev and Fridovich (13) noted that "nitro blue tetrazolium can mediate $O_2^{\cdot-}$ production in systems that would not otherwise produce $O_2^{\cdot-}$." In this context, also a disagreement exists in the literature (11, 12) whether superoxide is formed by reaction 4. From their examination of the autoxidation of H4B models, methylated tetra- and dihydropterins, Bruice and coworkers (14) proposed that in the initial, rate-controlling electron-transfer step a ($H4B^{\cdot+}$, $O_2^{\cdot-}$) radical pair should be produced, which instantaneously collapses to a hydroperoxide intermediate rather than releasing a superoxide/hydroperoxyl radical. The fact that no H_2O_2 formation could be detected apparently supported this hypothesis, however, the authors already noted that H_2O_2 could have been consumed by subsequent, direct reaction with the H4B model compounds. The idea that H4B directly reduces oxygen to $O_2^{\cdot-}$ was revived in 1993 when production of H_2O_2 was indeed monitored, but found to be partly inhibited by Cu,Zn-SOD (15). Later, the capability of H4B to decrease nitric oxide levels in the presence of oxygen, and the observed inhibitory effect of Cu,Zn-SOD on this process, provided a further, strong argument for the intermediate release of $O_2^{\cdot-}$ during tetrahydrobiopterin autoxidation,

* This work was supported by the Stiftung VERUM. The costs of publication of this article were defrayed in part by the payment of page charges. This article must therefore be hereby marked "*advertisement*" in accordance with 18 U.S.C. Section 1734 solely to indicate this fact.

§ To whom correspondence should be addressed: Institut für Physiologische Chemie, Universitätsklinikum Essen, Hufelandstr. 55, D-45122 Essen, Germany. Tel.: 49-201-723-4107; Fax: 49-201-723-5943; E-mail: michael.kirsch@uni-essen.de.

[1] The abbreviations used are: H4B or tetrahydrobiopterin, 2-amino-*6R*-(*1R*,*2S*-dihydroxypropyl)-5,6,7,8-tetrahydro-4(*1H*)-pteridinone; dihydrobiopterin or H2B, 2-amino-*6*-(*1R*,*2S*-dihydroxypropyl)-7,8-dihydro-4(*1H*)-pteridinone; dihydropterin or H2P, 7,8-dihydro-4(*1H*)-pteridinone; NOS, nitric-oxide synthase; peroxynitrite, $ONOO^-$/ONOOH equilibrium mixture; lucigenin, bis-*N*-methylacridinium; DEPMPO, 5-(diethoxyphosphoryl)-5-methyl-pyrroline *N*-oxide; FNOCT-1, fluorescence nitric oxide cheletropic trap.

thereby producing peroxynitrite (16). Taken together, the foregoing observations, especially with regard to the inhibitory effects of Cu,Zn-SOD, leave little doubt that $O_2^{\cdot-}$ is involved in the autoxidation of H4B and related compounds. However, in none of these papers was free $O_2^{\cdot-}$ directly and unequivocally identified. On the contrary, the proposal that H4B generates free $O_2^{\cdot-}$ from molecular oxygen was later disputed by Xia and Zweier (17) because these authors were unable to detect the expected adduct of $O_2^{\cdot-}$ to the spin trap compound DMPO, DMPO–OOH, by ESR spectrometry. As H4B was found to react quite fast with $O_2^{\cdot-}$ ($k = 3.9 \times 10^5$ M^{-1} s^{-1}) (18) it was referred to as a "superoxide scavenger." As a consequence, the possibility that $O_2^{\cdot-}$ is non-enzymatically generated from reaction of H4B with dioxygen virtually vanished from the recent literature and its possible influence on the mechanisms of NOS activity is no longer discussed.

In the present study, we therefore reinvestigated the autoxidation of H4B with the aim to bring this issue back to the mind of the scientific community and to get better insight in the reaction mechanism and kinetics. The intermediacy of free $O_2^{\cdot-}$ from reaction of H4B with molecular oxygen is unequivocally proven. We fully confirm earlier hypotheses that a slow, one-electron transfer from H4B to O_2 very likely represents the initiation step for the consecutive, fast reaction of the thus formed $O_2^{\cdot-}$ with H4B, thereby setting up a chain process in which molecular oxygen is additionally converted to superoxide via reaction with the intermediary H3B$^{\cdot}$ radical. Hence, H4B indeed acts both as superoxide generator and as superoxide scavenger (19, 20). Further experiments show that the so formed superoxide is available for reaction with simultaneously produced nitric oxide.

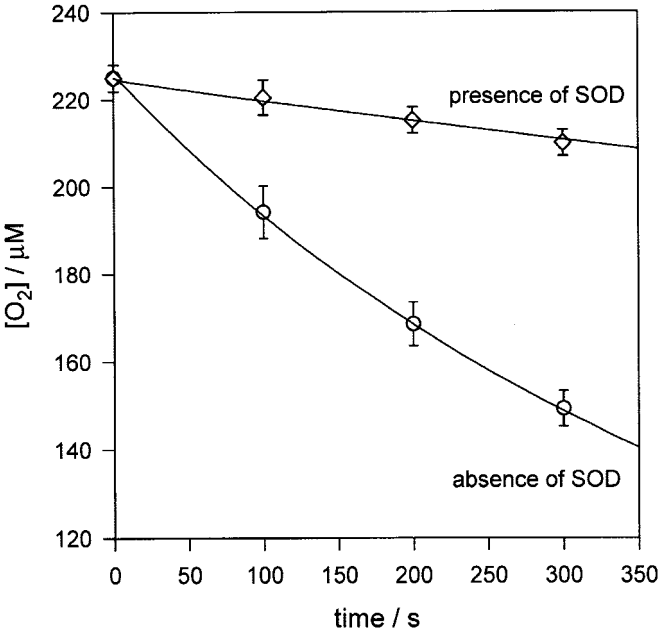

FIG. 1. **Effect of superoxide dismutase on O_2 consumption by tetrahydrobiopterin.** Tetrahdrobiopterin (600 μM) was added under normoxic conditions to 50 mM potassium phosphate buffer (37 °C, pH 7.5) containing 1300 units/liter of catalase in the absence and presence of 500 units/ml Cu,Zn-SOD. O_2 was measured polarographically with a Clark-type electrode. Data are mean ± S.D. of six independent experiments. Continuous traces are the simulated concentration-time profiles according to Table I. *Upper trace*, reactions 1–7; *lower trace*, reactions 1–9.

EXPERIMENTAL PROCEDURES

Materials—Catalase from beef liver (EC 1.11.1.6) and copper-zinc superoxide dismutase from bovine erythrocytes (EC 1.15.1.1) were obtained from Roche Diagnostics. Lucigenin and hydrogen peroxide were from Sigma. DEPMPO, H4B, H2B, and sepiapterin were purchased from Calbiochem-Novabiochem (Schwalbach, Germany). Commercially available mixtures of oxygen 5.0 and nitrogen 5.0 (20.5% O_2, 79.5% N_2, "synthetic air") and commercially available mixtures of oxygen 5.0, nitrogen 5.0, and carbon dioxide 4.6 (20.5% O_2, 74.5% N_2, 5% CO_2) were purchased from Messer-Griessheim (Oberhausen, Germany; 5.0 and 4.6 mean purities of 99.999 and 99.996%, respectively). All other chemicals were of the highest purity commercially available. The program "Chemical Kinetics Simulator 1.01" was kindly donated by International Business Machines Corporation.[2]

Solutions—Phosphate buffer solutions (50 mM) were treated with the heavy metal scavenger resin Chelex 100 (0.3 g in 10 ml) by gently shaking for 18 h in the dark. After low speed centrifugation for 5 min, the solutions were carefully decanted from the resin. The resin treatment resulted in an increase in pH by about 0.25 units. Various additives (Cu,Zn-SOD, DEPMPO, lucigenin, etc.) were then added. The pH was adjusted to 7.5 at 37 °C and the solutions were again bubbled (2 liters/min) with synthetic air or with the CO_2 mixture for 20 min. In the case of CO_2 bubbling, the pH had to be readjusted to 7.5. The pterins (H4B and H2B) and PAPA-NONOate were prepared as ×100 stock solutions at 4 °C in 200 mM HCl and 10 mM NaOH, respectively, and used within 15 min.

Experimental Conditions—The experiments were performed in reaction tubes (2.0 ml, Eppendorf, Hamburg, Germany) by using the drop-tube Vortex mixer technique as described previously (21).

Determination of Tetrahydrobiopterin, Dihydrobiopterin, and Sepiapterin—Formation of H2B ($\epsilon_M = 6820$ M^{-1} cm^{-1}), H2P ($\epsilon_M = 5400$ M^{-1} cm^{-1}), and sepiapterin ($\epsilon_M = 1530$ M^{-1} cm^{-1}) were quantified spectrophotometrically at 330 nm (22) on a Specord S100 (Analytic Jena, Germany) diode array spectrometer. In control experiments H4B, H2B, and sepiapterin were additionally quantified by capillary zone electrophoresis on a Beckman P/ACE 5000 apparatus under the following conditions: fused silica capillary (60-cm effective length, 750μm internal diameter), hydrodynamic injection for 5 s, temperature 30 °C, voltage 18 kV, normal polarity, UV detection at 280 nm. As the electrolyte system a mixture of 20 mM sodium phosphate solution and H_3PO_4 (final pH 1.6) was used. To each sample 10 mM tryptophan ($\epsilon_M = 5600$ M^{-1} cm^{-1}) was added as internal standard.

Determination of H_2O_2 and of O_2—Hydrogen peroxide was quantified by the amount of O_2 released upon addition of catalase (1300 units/ml). O_2 was determined polarographically with a Clark-type oxygen electrode (Saur, Reutlingen, Germany). The equilibrium concentration of molecular oxygen at "normoxic" conditions was determined for each of the experimental series and amounted rather constantly to 225 ± 5 μM.

Determination of Nitric Oxide—Nitric oxide was quantified polarographically with a graphite nitric oxide-sensing electrode (World Precision Instruments, Berlin, Germany) or followed by fluorescence spectroscopy (FL 3095 diode array spectrometer, J&M, Aalen, Germany) after reaction with the fluorescence nitric oxide cheletropic trap FNOCT-1 as reported previously (23, 24).

Determination of Nitrate and Nitrite—The yields of nitrate and nitrite were quantified by the use of nitrate reductase in conjunction with the Griess assay. The Griess assay was carried out as described elsewhere (25).

Determination of Superoxide—Superoxide radical formation was established by using two independent methods. As a first method lucigenin-mediated luminescence was employed. Solutions of lucigenin (1 mM, pH 8, 50 mM potassium phosphate, 300 μl) were mixed with solutions of H4B (4 mM, 100 mM HCl, 5 μl). Light emission was followed with a Lumat LB 9507 luminometer (Berthold Technologies, Germany) set to an integration time of 1 s.

The second method for verification of superoxide formation was ESR spectrometry. ESR spectra were recorded at ambient temperature on a Bruker ESP-300E X-band spectrometer (Bruker, Rheinstetten, Germany) equipped with a TM_{110} wide bore cavity. Solutions were prepared from 1 ml of the buffer solution (pH 7.4) containing DEPMPO (100 mM). H4B (1 mM) was added to the foregoing solution by vortexing under aerobic conditions. The reaction mixtures were quickly transferred to an aqueous solution quartz cell (Willmad, Buena, NJ). The first spectra were run as fast as possible, *i.e.* within 1 min, and then in 13-min intervals. Recording conditions: microwave frequency, 9.8 GHz; modulation, 0.04 millitesla; signal gain, 5×10^5; sweep range, 20 millitesla; sweep time, 4 min. Spectrum simulation was performed using the WinSim program (26). Spectrum integration was carried out with the Bruker WinEPR software.

[2] www.almaden.ibm.com/st/msim.

TABLE I
Kinetic scheme for the simulation of oxygen consumption by tetrahydrobiopterin in the absence and presence of Cu,Zn-SOD

Entry	Reaction	$k/M^{-1}/s^{-1}$	Ref.
1	$H3B^{\cdot} + O_2 \rightarrow qH2B + O_2^{\cdot-} + H^+$	$3.2 (\pm 0.3) \times 10^3$	This work
2	$H4B + O_2 \rightarrow H3B^{\cdot} + O_2^{\cdot-} + H^+$	$0.60 (\pm 0.03)$	This work
3	$H4B + O_2^{\cdot-} + H^+ \rightarrow H3B^{\cdot} + H_2O_2$	3.9×10^5	18
4	$2\ H3B^+ \rightarrow qH2B + H4B$	9.3×10^4	39
5	$2\ O_2^{\cdot-} (+ 2\ H^+) \rightarrow H_2O_2 + O_2$	6.3×10^5	28
6	$H_2O_2 +$ catalase $\rightarrow$ compound 1	6×10^6	58
7	$H_2O_2 +$ compound 1 $\rightarrow O_2 + 2\ H_2O +$ catalase	3×10^7	58
8	$O_2^{\cdot-} + Cu^{2+}$, Zn-SOD $(+ 2\ H^+) \rightarrow Cu^+$,Zn-SOD	2×10^9	59
9	Cu^+,Zn-SOD $+ O_2^{\cdot-} \rightarrow O_2 + H_2O_2 + Cu^{2+}$,Zn-SOD	2×10^9	Estimated (60)

Kinetic Simulations of Tetrahydrobiopterin-dependent Nitric Oxide Consumption—The kinetic simulations were performed with the "Chemical Kinetic Software (CKS)" (IBM, Almaden Research Center, San Jose, CA) and the Kintecus program written by Dr. James C. Ianni.[3] The CKS software uses a stochastic approach to calculate concentration-time profiles from given rate constants, whereas Kintecus performs numerical integrations of the rate laws. The virtues of the latter program are that it runs incredibly fast on a standard PC and is basically unrestricted in terms of the number of reactions and species. Furthermore, the program automatically checks for correct mass and charge balance and also offers the opportunity to modify the concentration of selected compounds at any point on the time scale. This feature easily allowed to model the effect of adding H4B to a solution where $^{\cdot}NO$ is *in situ* generated by PAPA-NONOate in the presence of oxygen.

RESULTS

Influence of Superoxide Dismutase on Tetrahydrobiopterin Autoxidation—Davies and Kaufman (15) reported that H_2O_2 is formed from autoxidation of H4B. In line with these findings 55.7 ± 5 μM H_2O_2 was found when 600 μM H4B was incubated for 40 min at 37 °C in aerobic phosphate buffer solutions at pH 7.5 (three experiments performed in duplicate). As the formation of H_2O_2 should proceed at the expense of oxygen, oxygen uptake by H4B was followed in the presence of catalase (1300 units/liters) (to avoid possible oxidation of H4B by hydrogen peroxide (11)), and the effect of Cu,Zn-SOD on oxygen uptake was studied (Fig. 1). In agreement with data of both Pearson (8) as well as Heikkila and Cohen (10), oxygen was consumed by H4B. In the absence of Cu,Zn-SOD oxygen consumption proceeded with an apparent half-life of 8.4 min. Addition of Cu,Zn-SOD (500 units/ml) decreased H4B-dependent O_2 consumption by about 83%, corresponding to an apparent half-life of 50.3 min. Because the addition of Cu,Zn-SOD abolished the consecutive reaction between superoxide and tetrahydrobiopterin, the upper trace of Fig. 1 should reflect the overall rate constant for the oxidation of H4B, obeying the stoichiometry of reaction 1 under these conditions.

$$2\ H4B + O_2 \rightarrow 2\ H2B + 2\ H_2O \qquad \text{(Eq. 5)}$$

The rate constant for reaction of H4B with O_2 was estimated from kinetic simulation with the CKS software employing the reactions displayed in Table I by systematically varying the rate constants of entries 1 and 2 (Table I).

A best fit to the experimental data in the absence (Table I, entries 1–7) and presence of Cu,Zn-SOD (Table I, entries 1–9) was obtained with k(entry 2) $= 0.60 \pm 0.03$ $M^{-1}\ s^{-1}$ (Fig. 1). This value is in very good agreement with the value 1.44 ± 0.18 $M^{-1}\ s^{-1}$ as determined by Mayer *et al.* (16) for the conversion of H4B, which according to the stoichiometry of Equation 1 is twice as fast as the consumption of oxygen. The estimated rate constant k(entry 1) = of about 3×10^3 $M^{-1}\ s^{-1}$ for superoxide formation from reaction of the intermediary $H3B^{\cdot}$ radical with oxygen appears reasonable for this type of compound (28). Eberlein *et al.* (14) estimated values of k(entry 2)′ < 2.1 and k(entry 1)′ < 503 $M^{-1}\ s^{-1}$ for the corresponding rate constants of the H4B model compound 6,6,7,7-tetramethyl-5,6,7,8-tetrahydropterin. Because carbon-centered radicals generally react close to diffusion control with O_2 (28), rate constant k(entry 1) thus represents the overall process of the following reaction (Equation 6).

$$H3B^{\cdot} + O_2 = H3BOO^{\cdot} \rightarrow qH2B + O_2^{\cdot-} + H^+ \qquad \text{(Eq. 6)}$$

To further substantiate the inhibitory effect of superoxide dismutase toward tetrahydrobiopterin autoxidation, the accumulated formation of the various pterin-type products, *i.e.* sepiapterin, H2B, and dihydropterin (H2P), was monitored spectrophotometrically at 330 nm (where all products significantly absorb) (22) in the absence and presence of Cu,Zn-SOD. Formation of the various pterins from autoxidation of 20 μM H4B increased with increasing incubation time in an exponential manner (Fig. 2), with an apparent pseudo-first order rate constant of $(6.6 \pm 0.1) \times 10^{-4}\ s^{-1}$. Addition of Cu,Zn-SOD (100 units/ml) inhibited H4B autoxidation by a factor of five. From the pseudo-first order rate constant of $(1.36 \pm 0.05) \times 10^{-4}\ s^{-1}$ and an oxygen concentration of 225 μM, a rate constant of

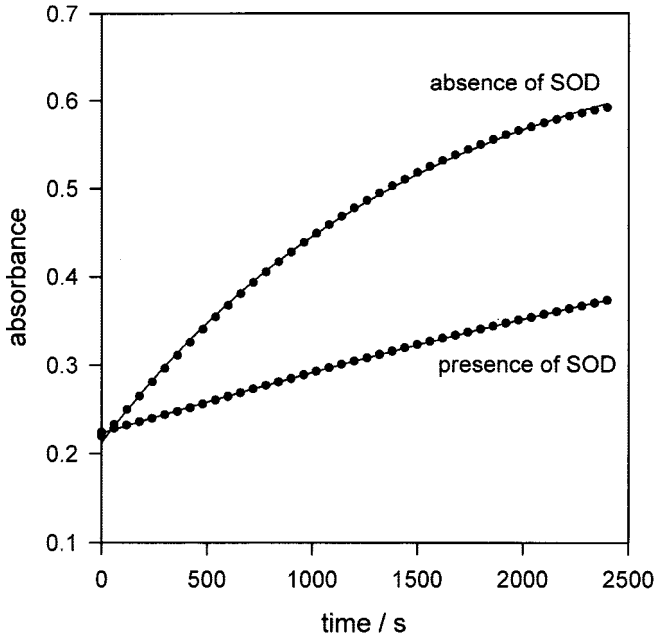

FIG. 2. **Effect of superoxide dismutase on formation of pterins from autoxidation of H4B.** Tetrahydrobiopterin (20 μM) was incubated under normoxic conditions in 50 mM potassium phosphate buffer (37 °C, pH 7.5) in the absence and presence of 625 nM Cu,Zn-SOD (100 units/ml). The time-dependent increase of the concentrations of dihydrobiopterin and dihydropterin, respectively, was followed by monitoring the optical density at λ = 330 nm ($\epsilon_M = 6820\ M^{-1}\ cm^{-1}$, $\epsilon_M = 5400\ M^{-1}\ cm^{-1}$) with a diode array spectrophotometer (scanning time 1 s). The data shown are representative of six similar experiments. The *continuous lines* are the least-squares fits to a first-order rate law.

[3] J. C. Ianni, 2.80 Ed., www.kintecus.com.

TABLE II
Yield of dihydrobiopterin from autoxidation of tetrahydrobiopterin

Tetrahydrobiopterin (330 μM) was added under normoxic conditions to 50 mM potassium phosphate buffer (37 °C, pH 7.5). After the selected time points autoxidation of tetrahydrobiopterin was stopped by adding HCl to reach a final pH of 4 and the contents of H4B, H2B, and sepiapterin, respectively, were measured chromatographically with a capillary zone electrophoresis apparatus. Data are mean ± S.D. of eight independent experiments.

Time	H4B	Consumed	H2B	Sepiapterin	Yield[a]
min			μM		%
0	329.8 ± 16	0.0	0.0 ± 0	0.0 ± 0	0
7	228.4 ± 11	101.4	56.9 ± 6	0.0 ± 0	56
15	144.7 ± 7	185.1	102.9 ± 11	0.0 ± 0	56
20	108.1 ± 1	221.7	102.1 ± 8	19.9 ± 4	56

[a] Yield (%) = ((H_2B + sepiapterin) / consumed) × 100.

0.60 ± 0.02 M^{-1} s^{-1} was derived, in excellent agreement with the above oxygen uptake experiments. As the formation of H2B from autoxidation of H4B was sometimes questioned (29), its formation was established by capillary zone electrophoresis by spiking with authentic material (Table II). In full agreement with data of Davies *et al.* (22), H2B was produced during autoxidation of H4B. At longer incubation periods sepiapterin was additionally produced, at the expense of H2B. H2P accounted for the mass balance difference (about 45%), but was not independently quantified. Plots of the data of Table II *versus* time (data not shown) showed an apparent exponential behavior for the decrease of H4B and the formation of H2B + H2P + sepiapterin, respectively, with a half-life of 12.8 min under these conditions. With regard to the lower H4B concentration compared with the conditions of Fig. 1, this half-life is in good agreement with the half-life of oxygen uptake. The observation that 56% of the consumed H4B was oxidized to H2B points to the intermediacy of the quinonoid form of dihydrobiopterin, qH2B, because Davies *et al.* (22) found that this intermediate ($t_{1/2}$ = 1–2 min) isomerizes under similar experimental conditions with a yield of 55.1% to H2B. The inhibitory action of Cu,Zn-SOD was not further significantly increased by increasing its activity 10-fold, and H4B was found to be stable under oxygen-free (hypoxic) conditions (data not shown). Combined, the foregoing observations strongly indicated that free superoxide is formed from direct reaction of H4B and molecular oxygen and that the initially formed superoxide further accelerated autoxidation of H4B by a factor of 5 to 6.

Consumption of Nitric Oxide by Tetrahydrobiopterin/Oxygen—Mayer and co-workers (16) have reported that nitric oxide is consumed by H4B in the presence of molecular oxygen and attributed this correctly to the intermediacy of peroxynitrite. In this case nitrate and nitrite plus O_2 must be produced, their relative yields strongly varying with pH around pH 7.5 (Equations 7–9) (30),[4,5]

$$H4B + O_2 \rightarrow H4B^{\ddagger} + O_2^{\cdot-} \quad \text{(Eq. 7)}$$

$$O_2^{\cdot-} + {}^{\cdot}NO \rightarrow ONOO^- \quad \text{(Eq. 8)}$$

$$ONOO^- \rightarrow NO_3^-/NO_2^- + O_2 \quad \text{(Eq. 9)}$$

In fact, ·NO released from the nitric oxide donor PAPA-NONOate (10 μM) in air-saturated buffer was instantaneously consumed by added H4B (10–50 μM) (Fig. 3*A*). The decrease of the level of nitric oxide after addition of H4B proceeded in a biphasic manner, implying that two kinetically different ·NO consuming routes are followed under the applied experimental conditions. To check on this, the concentration-time profiles were simulated with the Kintecus program by employing the reactions collected in Table III. Despite the large number of reactions, the H4B-dependent uptakes of nitric oxide are excellently reproduced (Fig. 3*B*). Thus, the consumption of ·NO can be satisfactorily explained by the intermediary action of superoxide. In line with this conclusion, the H4B-dependent decrease of the ·NO concentration was largely abolished in the presence of 5000 units/ml Cu,Zn-SOD (data not shown), in full agreement with observations reported by Mayer *et al.* (16).

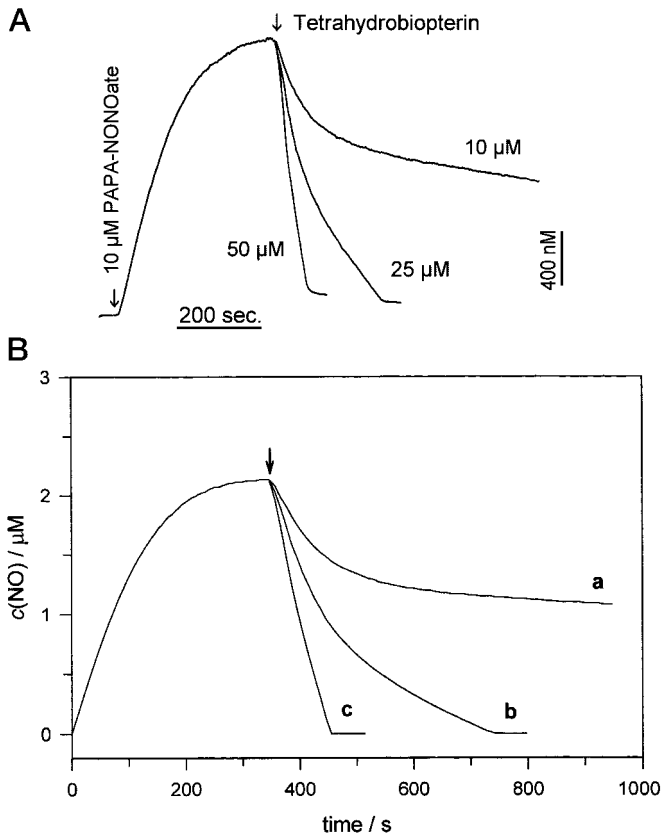

FIG. 3. **Tetrahydrobiopterin/oxygen-dependent consumption of nitric oxide.** *A*, PAPA-NONOate (10 μM) was dissolved in 50 mM potassium phosphate buffer (37 °C, pH 7.5) and the release of ·NO was monitored with a nitric oxide electrode. At the maximum of the nitric oxide peak, a solution of tetrahydrobiopterin (10–50 μM final concentrations) was added. The shown traces are representative of six similar experiments. *B*, kinetic simulation of the concentration-time profiles of *A* with the computer program Kintecus using the reactions outlined in Table III.

Additional experiments were performed with the fluorescence nitric oxide cheletropic trap FNOCT-1 (23, 24), which specifically measures the integrated (total) amount of released nitric oxide by converting it into a stable, fluorescent adduct, FNOCT-NOH. The production of ·NO from 50 μM PAPA-NONOate in oxygen-free phosphate buffer (pH 7.2) and in the presence of H4B (1 mM), FNOCT-1 (50 μM), and Cu,Zn-SOD (200 units/ml), as monitored by the growth of the fluorescence of FNOCT-NOH, is displayed in trace A of Fig. 4. The half-life of the fluorescence growth ($t_{1/2}$ ~ 74 min) is in good agreement with the published half-life for decomposition of PAPA-NONOate (31) under similar conditions. An identical time profile was observed in the absence of Cu,Zn-SOD (data not shown). However, under aerobic conditions (air-saturated buffer) and in the absence of Cu,Zn-SOD, the FNOCT-NOH fluorescence is

[4] M. Kirsch, H.-G. Korth, A. Wensing, R. Sustmann, and H. de Groot, unpublished observations.

[5] Peroxynitrite-mediated formation of NO_3^-/NO_2^- + O_2 reflected a highly complicated process that is initiated by the hydroxyl radical as displayed in Table III, entries 3, 5, 6, 7, 8, 28, and 37.

TABLE III
Elementary reactions and rate constants used in the kinetic simulation of tetrahydrobiopterin-dependent consumption of nitric oxide

Entry	Reaction[a]	k[b]	Refs.	Remarks
		$M^{-1}\,s^{-1}$; s^{-1}		
1	$O_2^- + {}^{\cdot}NO \rightarrow ONOO^-$	4.8×10^8	59	
2	$H4B + O_2 \rightarrow H4B^{+\cdot} + O_2^-$	0.6		This paper
3	$ONOO^- + H_3O^+ \rightarrow ONOOH + H_2O$	5×10^{10}	61	Estimated
4	$ONOOH + H_2O \rightarrow ONOO^- + H_3O^+$	1.43×10^2		From entry 3 and $pK_s = 6.8$
5	$ONOOH \rightarrow HNO_3$	0.94	62	72% of 1.3 s^{-1}, 37 °C
6	$ONOOH \rightarrow {}^{\cdot}NO_2 + HO^{\cdot}$	0.36	63	28% of 1.3 s^{-1}, 37 °C
7	$ONOO^- + HO^{\cdot} \rightarrow O_2 + {}^{\cdot}NO + HO^-$	4.8×10^9	64	
8	$ONOOH + HO^{\cdot} \rightarrow O_2 + {}^{\cdot}NO + H_2O$	2×10^7		Estimated, similar to H_2O_2
9	$NO_2^- + HO^{\cdot} \rightarrow HO^- + {}^{\cdot}NO_2$	5.3×10^9	65	
10	$2\,HO^{\cdot} \rightarrow H_2O_2$	5.5×10^9	59	
11	$H_2O_2 + HO^{\cdot} \rightarrow HOO^{\cdot} + H_2O$	2.7×10^7	59	
12	$2\,HOO^{\cdot} \rightarrow H_2O_2 + O_2$	8.6×10^5	59	
13	$HOO^- + HO^{\cdot} \rightarrow HOO^{\cdot} + HO^-$	7.5×10^9	59	
14	$2\,O_2^- + H_2O \rightarrow O_2 + HOO^- + HO^-$	63	59	
15	$HOO^{\cdot} + O_2^- \rightarrow HOO^- + O_2$	9.7×10^7	59	
16	$HO^{\cdot} + {}^{\cdot}NO \rightarrow HNO_2$	1×10^{10}	59	
17	$HO^{\cdot} + {}^{\cdot}NO_2 \rightarrow HNO_3$	4.5×10^9	59	
18	$HO^{\cdot} + {}^{\cdot}NO_2 \rightarrow ONOOH$	4.5×10^9		From k(17 + 18) = 1×10^{10} $k(17)/k$ (18) = 1:1
19	$HOO^{\cdot} + {}^{\cdot}NO \rightarrow ONOOH$	3.2×10^9	59	
20	$HOO^{\cdot} + {}^{\cdot}NO_2 \rightarrow O_2NOOH$	4×10^9	59	
21	$O_2^- + {}^{\cdot}NO_2 \rightarrow O_2NOO^-$	4.5×10^9	59	
22	$H_2O_2 + H_2O \rightarrow HOO^- + H_3O^{\cdot}$	3.2×10^{-3}		From entry 23 and $pK_s = 11.75$
23	$HOO^- + H_3O^+ \rightarrow H_2O_2 + H_2O$	5×10^{10}	61	Estimated
24	$H_3O^{\cdot} + NO_2^- \rightarrow HNO_2 + H_2O$	5×10^{10}	61	Estimated
25	$HNO_2 + H_2O \rightarrow H_3O^+ + NO_2^-$	7.2×10^5		From entry 24 and $pK_s = 3.1$
26	$H_3O^+ + O_2NOO^- \rightarrow O_2NOOH + H_2O$	5×10^{10}	61	Estimated
27	$O_2NOOH + H_2O \rightarrow O_2NOO^- + H_3O^+$	1.43×10^3		from entry 26 and $pK_s = 5.8$
28	${}^{\cdot}NO + {}^{\cdot}NO_2 \rightarrow N_2O_3$	1.1×10^9	59	
29	$N_2O_3 \rightarrow {}^{\cdot}NO + {}^{\cdot}NO_2$	8.0×10^4	66	
30	$2\,{}^{\cdot}NO_2 \rightarrow N_2O4$	4.5×10^8	59	
31	$N_2O_4 \rightarrow 2\,{}^{\cdot}NO_2$	6.9×10^3	66	
32	$HOO^{\cdot} + H_2O \rightarrow O_2^- + H_3O^+$	1.4×10^4		From entry 33 and $pK_s = 4.8$
33	$O_2^- + H_3O^+ \rightarrow HOO^{\cdot -} + H_2O$	5×10^{10}	61	Estimated
34	$O_2NOO^- \rightarrow NO_2^- + O_2$	1.4	67	
35	$O_2NOOH \rightarrow HNO_2 + O_2$	7.0×10^{-4}	68	
36	$O_2NOOH \rightarrow HOO^{\cdot} + {}^{\cdot}NO_2$	5×10^{-2}	69	
37	$N_2O_3\,(+\,H_2O) \rightarrow 2\,HNO_2$	$2 \times 10^3 + 10^8 \times [HO^-]$	66	
38	$N_2O_3\,(+\,H_2O) \rightarrow 2\,HNO_2$	$2 \times 10^3 + 8 \times 10^5 \times [HPO4^{2-}]$	70	
39	$2\,HNO_2 \rightarrow N_2O_2 + H_2O$	13.4	71	
40	$N_2O_4\,(+\,H_2O) \rightarrow HNO_3 + HNO_2$	1×10^3	66	
41	$N_2O_3 + ONOO^- \rightarrow NO_2^- + 2\,{}^{\cdot}NO_2$	3.1×10^8	65	
43	$HO^{\cdot} + O_2^- \rightarrow O_2 + HO^-$	1.1×10^{10}	59	
44	$HNO_2 + H_3O^+ \rightarrow NO^+ + 2\,H_2O$	5.9×10^1	72	
45	$O_2NOO^- \rightarrow NO^{\cdot} + O_2^-$	1.05	67	
46	$2\,{}^{\cdot}NO + O_2 \rightarrow 2\,{}^{\cdot}NO_2$	2.2×10^8	73	
47	$NO^+ + H_2O \rightarrow HNO_2 + H^+$	1.1×10^{10}	74	
48	$HNO_3 + H_2O \rightarrow H_3O^+ + NO_3^-$	2×10^{10}		From entry 49 and $pK_s = -1.34$
49	$H_3O^+ + NO_3^- \rightarrow HNO_3 + H_2O$	5×10^{10}	61	Estimated
50	$NO^+ + HO^- \rightarrow HNO_2$	5×10^{10}	61	Estimated
51	PAPA-NONOate $\rightarrow$ products + 1.7 ${}^{\cdot}NO$	7.7×10^{-4}	27,31	
52	$H4B^{+\cdot} + H_2O \rightarrow H3B^{\cdot} + H_3O^+$	5.7×10^3		From entry 53 and $pK_s = 5.2$
53	$H3B^{\cdot} + H_3O^+ \rightarrow H4B^{\cdot +} + H_2O$	5×10^{10}	61	Estimated
54	$2\,H3B \rightarrow H4B + qH2B$	9.3×10^4	39	
55	$H3B^{\cdot} + O_2 \rightarrow H3BOO$	2×10^9		Estimated, similar to $NAD^{\cdot} + O_2$
56	$H3BOO^{\cdot} \rightarrow qH2B + H^+\,O_2^-$	3.2×10^3		This paper
57	$H4B + HO^{\cdot} \rightarrow H4B^{\cdot +} + HO^-$	8.8×10^9	39	
58	$H4B + {}^{\cdot}NO_2 \rightarrow H4B^{+\cdot} + NO_2^-$	9.4×10^8	39	
59	$H4B + O_2^- \rightarrow H3B^{\cdot} + HOO^-$	3.9×10^5	18	

[a] Not sorted to logical order.
[b] At ambient temperature (20-25°C) or 37° C.

largely suppressed (trace B), in accord with a rapid reaction of ·NO with superoxide. This was confirmed by prior addition of Cu,Zn-SOD to the reaction mixture. Now a similar ·NO production is monitored as in the absence of oxygen (trace C).

Under aerobic conditions, nitrite was found to be the sole oxidation product from PAPA-NONOate-released ·NO in the absence of H4B (Fig. 5*A*) (32). Hence, detection of nitrate in the presence of H4B would further support the proposed intermediacy of peroxynitrite according to Equations 7–9. In fact, the yield of nitrate from decay of 100 μM PAPA-NONOate increased with increasing concentrations of H4B in an apparent exponential manner (Fig. 5*A*). Production of nitrite decreased simultaneously in an inverse relationship, *i.e.* there appears to be an increased production of nitrate at the expense of nitrite. Both yields level out at 82 μM, corresponding to about half the yield of NO_2^- in the absence of H4B. The rate constants for Cu,Zn-SOD-catalyzed superoxide dismutation and reaction of superoxide with ·NO are of similar magnitude. Therefore, the yields of both nitrate and nitrite from reaction mixtures of 200 μM H4B and 100 μM PAPA-NONOate in aerated phosphate buffer were not markedly affected at Cu,Zn-SOD activities lower than 100 units/ml (Fig. 5*B*). However, as expected, the

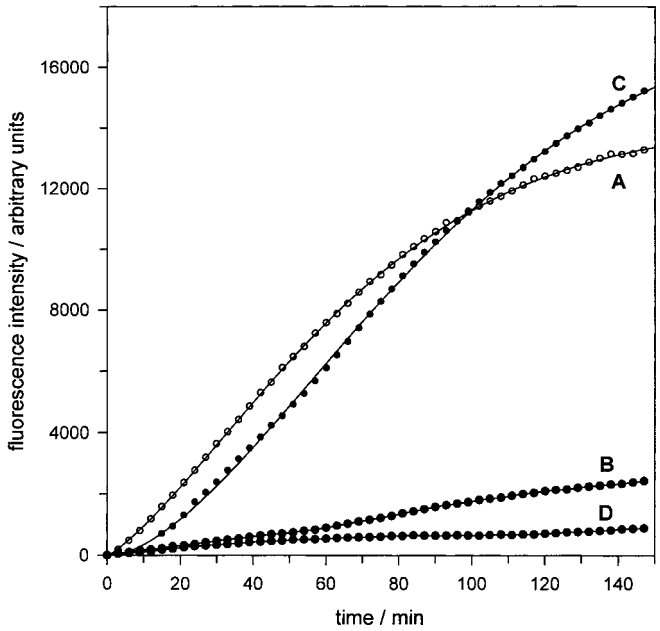

FIG. 4. **Effect of oxygen and Cu,Zn-SOD on tetrahydrobiopterin-dependent consumption of nitric oxide.** PAPA-NONOate (50 μM) was dissolved in 50 mM potassium phosphate buffer (25 °C, 1 mM H4B, pH 7.25) in the absence and presence of 225 μM oxygen and the release of $^{\cdot}$NO was monitored with FNOCT-1 (50 μM). *A*, oxygen-free phosphate buffer in the presence of Cu,Zn-SOD (200 units/ml). *B*, aerobic conditions (air-saturated buffer) in the absence of Cu,Zn-SOD. *C*, aerobic conditions (air-saturated buffer) in the presence of Cu,Zn-SOD (200 units/ml). *D*, aerobic conditions (air-saturated buffer) as described in *C* but in the absence of PAPA-NONOate.

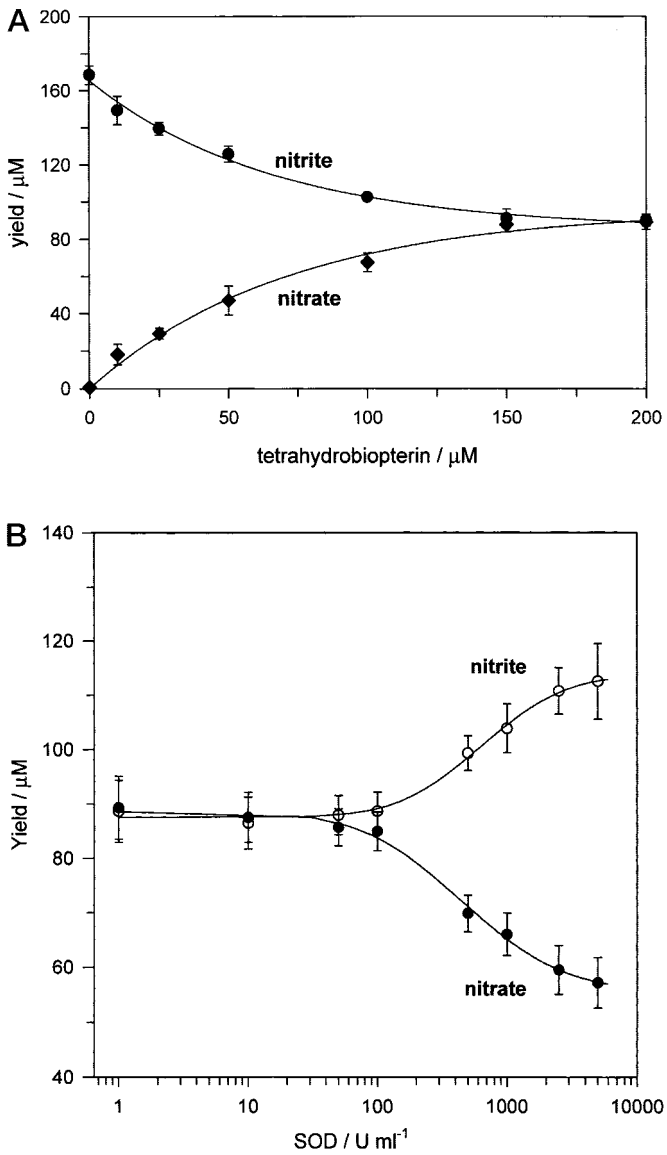

FIG. 5. **Tetrahydrobiopterin-dependent formation of nitrate.** *A*, PAPA-NONOate (100 μM) and various concentrations of tetrahydrobiopterin in potassium phosphate buffer (50 mM, pH 7.5, 37 °C) were incubated for 2 h. Formation of nitrate/nitrite were quantified with the Griess assay in the absence (nitrite) and presence (nitrate + nitrite) of nitrate reductase. Each value represents the mean ± S.D. of three experiments performed in duplicate. *B*, PAPA-NONOate (100 μM), tetrahydrobiopterin (200 μM), and various activities of Cu,Zn-SOD in potassium phosphate buffer (50 mM, pH 7.5, 37 °C) were incubated for 2 h and the generation of both nitrate and nitrite were quantified with the Griess assay in the presence and absence of nitrate reductase. Each value represents the mean ± S.D. of three experiments performed in duplicate.

yield of nitrite increased at the expense of the nitrate yield at higher (≥100 units/ml) Cu,Zn-SOD activities by increased trapping of the intermediary $O_2^{\cdot-}$.

Detection of Superoxide from Tetrahydrobiopterin—Although the results presented so far already convincingly indicated the intermediacy of $O_2^{\cdot-}$ during autoxidation of H4B, further, and more direct evidence for superoxide formation was sought. In a first attempt, H4B was tested for its capability to induce light emission from lucigenin, a compound that is known to elicit luminescence on reaction with superoxide (33, 34). Indeed, a strong emission of light was observed when 66 μM H4B was added to lucigenin (1 mM) (Fig. 6). Presence of 100 units/ml Cu,Zn-SOD completely abolished the H4B-induced luminescence. Thus, intermediate formation of $O_2^{\cdot-}$ is very likely.

As the lucigenin luminescence method is an indirect assay for $O_2^{\cdot-}$ formation and because superoxide may be artificially produced by lucigenin itself (35–37), we further attempted to detect superoxide directly by scavenging with a nitrone-type spin trap compound, thereby (hopefully) generating a characteristic, ESR-detectable spin trap-$O_2^{\cdot-}$ adduct radical. ESR observation of a $-OO^{-}/^{-}OOH$-substituted nitroxyl radical would unequivocally prove the intermediacy of $O_2^{\cdot-}$. Xia and Zweier (17) were unable to detect ESR signals of the $O_2^{\cdot-}/HOO^{\cdot}$ adduct radical from interaction of H4B and oxygen by employing the commonly used spin trap compound DMPO (see Introduction). Unfortunately, in this case the use of DMPO may not have been an optimal choice for detecting $O_2^{\cdot-}$, as the half-life of the DMPO-OOH adduct radical is relatively short ($t_{1/2}$ ~ 1–2 min) (38). Hence, its stationary concentration may have stayed beyond the detection level of ESR because the rate of $O_2^{\cdot-}$ formation from H4B turned out to be relatively low (see above) in competition with its further, effective consumption by H4B (see "Discussion"). Therefore, we selected the phosphorylated nitrone compound DEPMPO as a spin trap. The DEPMPO-OOH adduct radical can be more easily detected by ESR spectrometry because of its significantly longer half-life ($t_{1/2}$ ~ 8 min) and an increased superoxide trapping rate (38).

In the absence of H4B a very weak background signal of the DEPMPO-OH adduct was detected from 100 mM DEPMPO in air-saturated phosphate buffer (pH 7.4) (Fig. 7, *trace A*). About 1 min after addition of H4B (to give a final concentration of 1 mM), the build-up of the characteristic ESR signals of the DEPMPO-OOH radical could be detected (Fig. 7, *trace B*). These signals increased with time, accompanied by the growth of signals of the DEPMPO-OH adduct radical and the (unspecified) adduct radical(s) of (a) carbon-centered radical(s) (DEPMPO-CX_n), as indicated by the typical β-H hyperfine

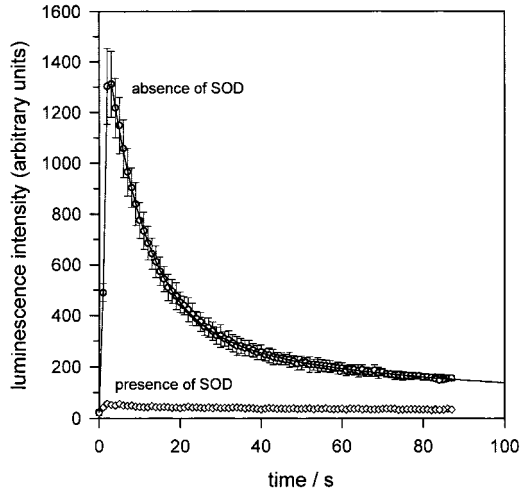

FIG. 6. **Verification of tetrahydrobiopterin-dependent formation of superoxide by eliciting of luminescence from lucigenin.** Tetrahydrobiopterin (66 μM) was added to lucigenin (1 mM) in 50 mM potassium phosphate buffer (25 °C, pH 8.0) in the absence and presence of 625 nM SOD (100 units/ml). Light emission was detected with a luminometer in the wavelength range 290–660 nm. Each value represents the mean ± S.D. of three experiments performed in duplicate. The *solid line* is the least-squares fit ($r^2 = 0.9997$) to a bi-exponential decay with $k_1 = 0.108 \pm 0.003$ and $k_2 = (1.85 \pm 0.62) \times 10^{-2}$ s^{-1}.

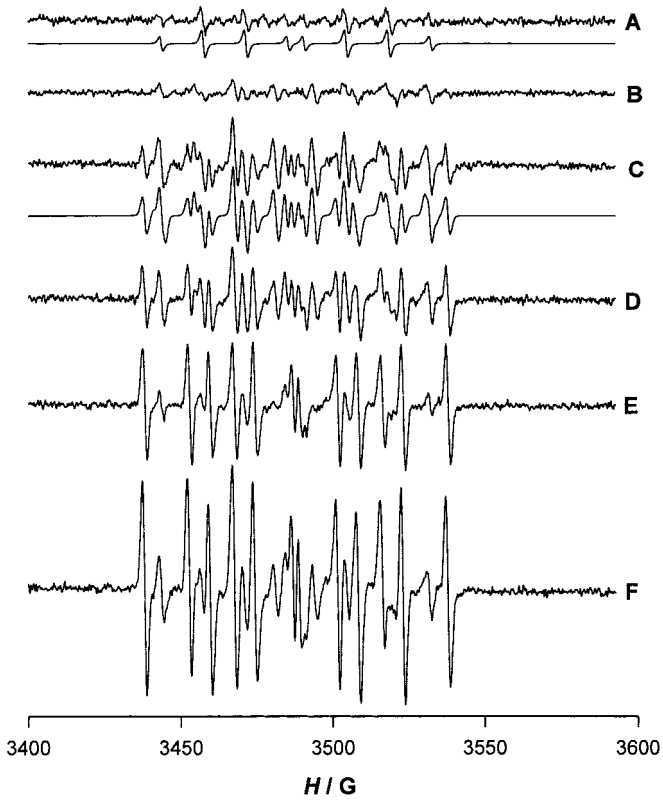

FIG. 7. **Direct verification of formation of superoxide from autoxidation of tetrahydrobiopterin by ESR spin trapping experiments.** ESR spectra were recorded after rapid mixing of solutions of DEPMPO (100 mM) and H4B (1 mM) in air-saturated potassium phosphate buffer (50 mM, pH 7.5) at room temperature. Recording conditions: microwave frequency, 9.87 GHz; modulation, 0.04 millitesla; signal gain, 5×10^5; sweep range, 20 millitesla; sweep time, 4 min. *A*, control, fresh DEPMPO in the absence of H4B 2 min after dissolution. The simulation shows the ESR spectrum of the DEPMPO-OH adduct radical with a(N) = 14.11, a(H) = 13.33, a(P) = 49.46 G; g = 2.0059. *B*, 2 min after mixing with H4B solution. *C*, 4 min after mixing. The simulation shows the superposition of the ESR spectra of DEPMPO-OH, the two conformers of DEPMPO-OOH with a(N) = 13.17, a(H) = 11.98, a(P) = 51.74 G, and a(N) = 13.13, a(H) = 1073, a(P) = 49.64 G; g = 2.005, and DEPMPO-CX$_n$ with a(N) = 14.85, a(H) = 21.51, a(P) = 48.70 G; g = 2.005. *D*, 12 min after mixing. *E*, 34 min after mixing. *F*, 50 min after mixing, 2 min after air bubbling for 30 s. The given reaction times refer to the center of the spectra.

splitting of about 22 G (Fig. 7, *trace C*). Whereas the latter signals further increased, the ESR spectra of DEPMPO-OOH and DEPMPO-OH again decreased (Fig. 7, *trace D–E*) with increasing reaction time. The time evolution of the integrated (from best-fit simulated spectra) ESR signal intensities of the spin adducts (Fig. 8) shows the DEPMPO-superoxide adduct going through a maximum value at about 8 min after addition of H4B, followed by a complete decay within 40 min. The signal intensity of DEPMPO-OH also goes through a maximum value (at about 12 min) but then remains almost constant at longer times. The time dependence of the DEPMPO-CX$_n$ signal clearly followed a sigmoid fashion to approach a saturation value after 40 min. This plateau value, as well as the complete disappearance of the DEPMPO-OOH radical indicated the consumption of the dissolved oxygen in the closed sample cell within this reaction period. In agreement, after bubbling of the reaction mixture with air for about 30 s, the DEPMPO-OOH spectrum again could be detected, together with further increased intensities of the DEPMPO-OH and DEPMPO-CX$_n$ spectra (Fig. 7, *trace E*). Similar ESR signal intensity-time profiles, but at higher signal intensities, were recorded from an oxygen-saturated reaction mixture (data not shown). In accord with the higher O_2 level in these experiments, the DEPMPO-OOH signal reached its maximum value faster, within 3 min, and could be monitored over a longer period of time (about 70 min). Likewise, the growth of the DEPMPO-CX$_n$ spectrum to its saturation value could be followed for about 80 min. As expected for a direct reaction of H4B with molecular oxygen, no significant build-up of ESR signals could be observed in the absence of O_2, *i.e.* from a mixture of H4B and DEPMPO in nitrogen-saturated phosphate buffer (Fig. 9, *traces A–C*) under otherwise identical conditions. The formation of $O_2^{\cdot-}$ from the H4B/O_2 interaction was further corroborated by the complete suppression of the DEPMPO-OOH ESR signal and strongly diminished DEPMPO-OH and DEPMPO-CX$_n$ signals in the presence of Cu,Zn-SOD (Fig. 9, *traces D–E*). The slight growth of these signals can reasonably be attributed to a slow oxidation of DEPMPO and H4B by the hydrogen peroxide produced from superoxide dismutation.

DISCUSSION

Our reinvestigation of the autoxidation of H4B presented here basically confirm earlier studies with respect to product formation (22), oxygen consumption (7, 10), nitric oxide consumption (16), kinetics (14, 16), and inhibitory effect of SOD (6, 15, 16). Beyond this, our ESR spin trapping experiments for the first time unequivocally prove that tetrahydrobiopterin reacts at physiological pH with molecular oxygen to produce *free* $O_2^{\cdot-}$ radicals. At first sight, this result seems to be in contradiction to recent reports that showed that H4B can act as a scavenger (reducing agent) for superoxide (18, 38–42).

From the data presented here it is understood that the initial step should be an electron transfer from H4B to O_2.

$$H4B + O_2 \rightarrow H4B^{\cdot+} + O_2^{\cdot-}\ k(6) = 0.60 \pm 0.03\ \text{M}^{-1}\ \text{s}^{-1} \qquad \text{(Eq. 10)}$$

The mechanisms by which a variety of radicals, *e.g.* $O_2^{\cdot-}$, $CO_3^{\cdot-}$, $^{\cdot}NO_2$, $HO^{\cdot}$, and $GS^{\cdot}$, oxidize H4B have been elucidated (18, 39). Superoxide has been proposed to react according the following reaction sequences.

$$O_2^{\cdot-} + H4B + 2\ H^+ \rightarrow H_2O_2 + H4B^{\cdot+} \qquad \text{(Eq. 11)}$$

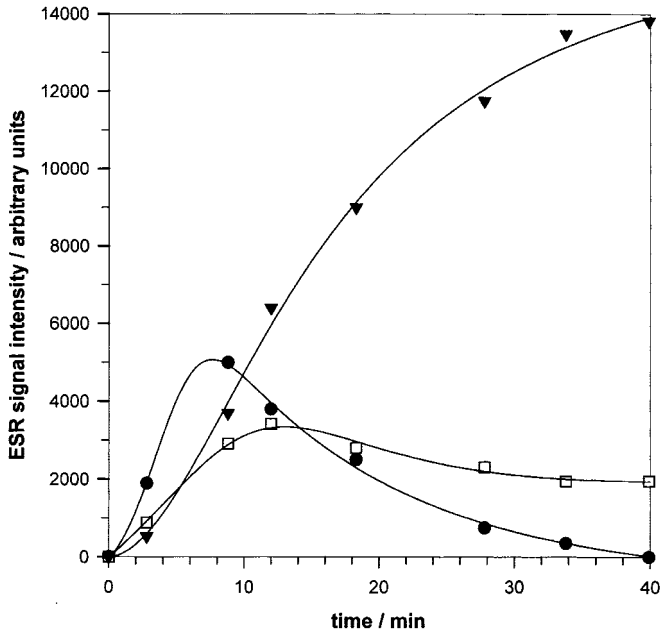

FIG. 8. **Time evolution of the DEPMPO spin adducts from autoxidation of tetrahydrobiopterin.** Time dependence of the integrated signal intensities of the ESR spectra of the DEPMPO radical adducts shown in Fig. 7. Signal intensities were obtained from numerical double integration of best-fitted simulated spectra using the hyperfine splittings given in the legend to Fig. 7. *Filled circles*, DEPMPO-OOH; *open squares*, DEPMPO-OH; *filled triangles*, DEPMPO-CX_n. The *solid lines* are empirical fits to the data points and are only intended to guide the eye.

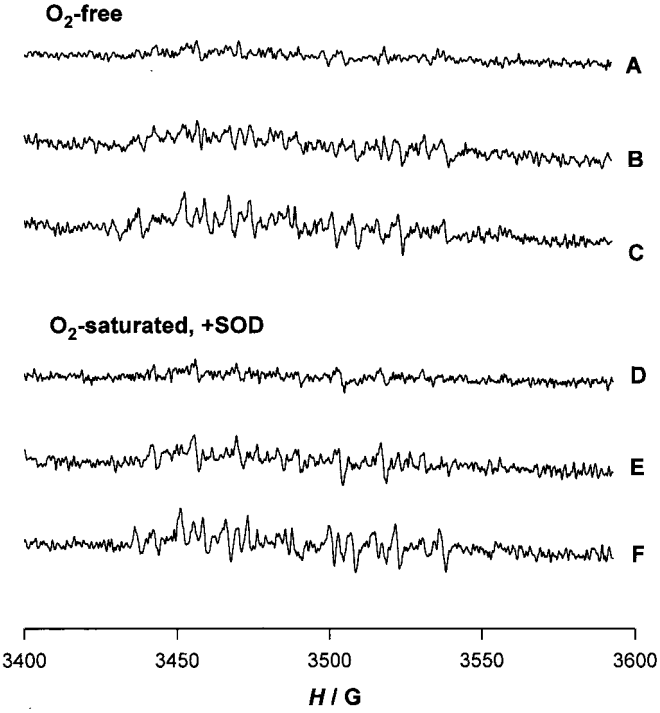

FIG. 9. **Further evidence for superoxide formation from autoxidation of tetrahydrobiopterin.** *A–C*, ESR spectra recorded after rapid mixing of solutions of DEPMPO (100 mM) and H4B (1 mM) in nitrogen-saturated phosphate buffer (pH 7.5, 50 mM). *A*, 1.5 min; *B*, 15 min; *C*, 37 min after mixing. *D–F*, ESR spectra recorded after rapid mixing of solutions of DEPMPO (100 mM) and H4B (1 mM) in air-saturated phosphate buffer (pH 7.5, 50 mM) in the presence of Cu,Zn-SOD (500 units/ml). *D*, 2 min; *E*, 26 min; *F*, 65 min after mixing. The reaction times refer to the center of the spectra. The small signals in spectra *E* and *F* are because of the DEPMPO-OH and DEPMPO-CX_n radicals, respectively.

$$H4B^{\cdot+} \rightarrow H3B^{\cdot} + H^+ \ (pk_a = 5.2\ (39)) \qquad \text{(Eq. 12)}$$

$$2\ H3B^{\cdot} \rightarrow H4B + qH2B \qquad \text{(Eq. 13)}$$

$$qH2B \rightarrow H2B \qquad \text{(Eq. 14)}$$

According to this mechanism, $O_2^{\cdot-}$ acts as an one-electron oxidant for H4B, the produced radical cation of which, $H4B^{\cdot+}$, undergoes rapid deprotonation at neutral pH (39). Disproportionation of the $H3B^{\cdot}$ radical leads to the formation of a quinoid form (qH2B) of dihydrobiopterin, which further rearranges to the normal H2B structure (Scheme 1). Hence, in the absence of any other targets, $O_2^{\cdot-}$ formed by Equation 7 will then oxidize H4B according to Equations 11–14. It has been proposed, and is very likely (compare the kinetic simulations, Table I, above), that $O_2^{\cdot-}$ is additionally produced by (diffusion-controlled) reaction of the $H3B^{\cdot}$ radical with oxygen (7, 8, 12, 18).

$$H3B^{\cdot} + O_2 \rightarrow [H3BOO^{\cdot}] \qquad \text{(Eq. 15)}$$

$$[H3BOO^{\cdot}] \rightarrow qH2B + H^+\ O_2^{\cdot-} \qquad \text{(Eq. 16)}$$

Formation of $O_2^{\cdot-}$ rather than substantial formation of hydroperoxides/alcohols from reaction of carbon-centered radicals with O_2 is facilitated for electron donor-substituted (*i.e.* strongly nucleophilic) radicals, for which the lifetime of the initially formed peroxyl radical is short (28), *i.e.* for which k (16) is high compared with possible bimolecular reactions of the peroxyl radical. According to the molecular structure of H4B, this can be expected to be the case for $H3B^{\cdot}$.[6] Likewise, the formation of hydroperoxides from recombination of $H3B^{\cdot}$ and $O_2^{\cdot-}$ (Equation 17), as has been proposed by Eberlein *et al.* (14), appears to be disfavored, *i.e.* the equilibrium of this reaction is shifted to the left side.

$$H3B^{\cdot} + O_2^{\cdot-} = H3BOO^- (+H^+) \rightarrow H3BOOH \qquad \text{(Eq. 17)}$$

Consequently, it is very likely that an $O_2^{\cdot-}$-dependent propagation process (chain reaction), via Equations 11, 12, 15, and 16, is established after initiation of O_2 oxidation of H4B (Equation 10). In this cycle, one H4B molecule will have reduced one molecule of dioxygen to H_2O_2. (Note that epinephrine (43) as well as 6-hydroxydopamine (44) have been reported to be autoxidized by such a mechanism.) Because hydrogen peroxide further slowly oxidizes H4B to H2B (+ 2 H_2O), the overall stoichiometry of reaction 1 will finally be fulfilled. The consumption of H_2O_2 by H4B readily explains why sometimes H_2O_2 had not been detected after autoxidation of H4B (14, 45).

The situation presented here will have a strong impact on experimental systems involving nitric-oxide synthase. Because there is increasing evidence that NOS-dependent $O_2^{\cdot-}$ generation is effectively decreased by bound tetrahydrobiopterin (18, 38, 40, 41), H4B is generally added in such protocols to increase the NOS-derived yield of nitric oxide by decreasing the superoxide level. According to the above results, a maximal yield of

[6] From various ESR studies on the $H4B^{\cdot+}$ radical cation it has been concluded that the unpaired spin density is mainly located on nitrogen atom N-5 (see Refs. 14 and 18, and references cited therein). This is basically confirmed by quantum chemical density functional theory calculations (H.-G. Korth, M. Kirsch, unpublished results), which predict about 35% of the unpaired spin to reside on this position. However, sizable contributions (30 and 14%) of the unpaired spin density are also found on C-4a and the carbonyl oxygen, respectively. The situation is somewhat changed in the deprotonated radical, $H3B^{\cdot}$, where about 55% of the unpaired spin resides on N-5, with substantial contributions of C-8a (23%). Hence, reaction with O_2 is expected to occur primarily at these positions.

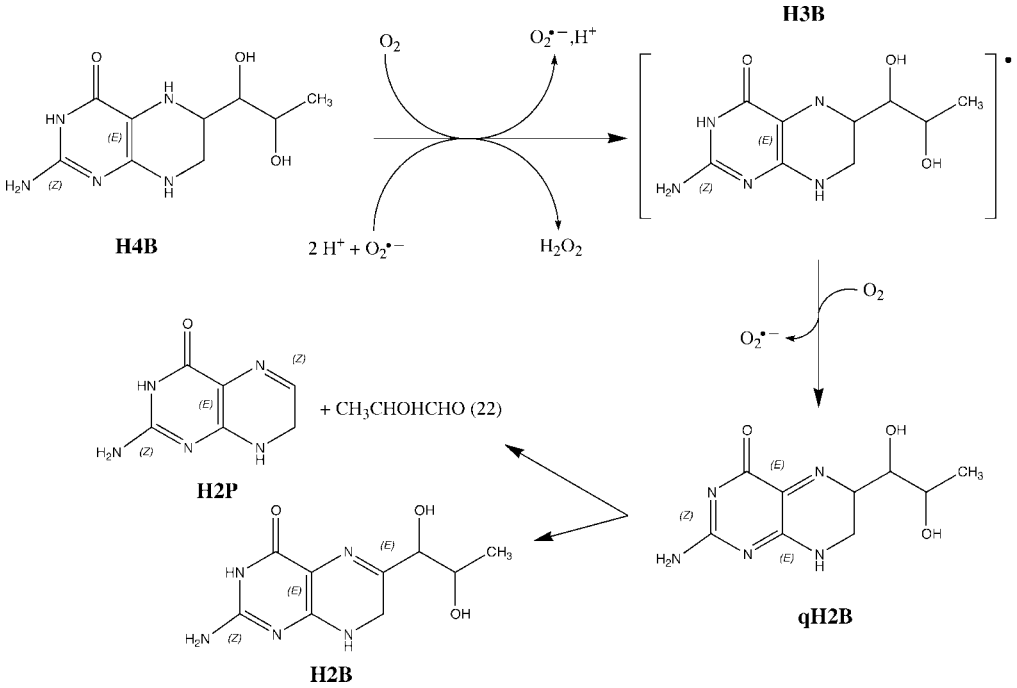

SCHEME 1. **Proposed reaction path.**

nitric oxide from NOS can only be achieved at an optimal H4B concentration, to avoid $O_2^{\bullet -}$ formation from either NOS-bound or freely diffusing tetrahydrobiopterin. At elevated $O_2^{\bullet -}$ fluxes the harmful oxidant peroxynitrite (Equation 8) is expected to be produced in a diffusion-controlled manner at the expense of nitric oxide.

The necessity of an optimal H4B concentration seems to be also highly important *in vivo*. Maintenance of physiological nitric oxide concentrations in illnesses with diseased arteries is today a major therapeutic goal and can be achieved by various strategies (46). One suggested improvement of such a clinical strategy is the supplementation of H4B. In full line with the view that protein-bound H4B increased eNOS-dependent $^{\bullet}NO$ generation (40), successful restoration of endothelial function by short term administration of tetrahydrobiopterin has been observed in patients with hypercholesterolemia (47), coronary artery disease (48), and atherosclerosis (48) as well as in smokers (49). Such beneficial effects of H4B administration strongly indicate that not enough endogenous tetrahydrobiopterin was available during these pathophysiological processes. On the other hand, there are also some indications that an endogenous up-regulation of H4B may additionally induce pathophysiological pathways via $O_2^{\bullet -}$. It is known that proinflammatory cytokines can up-regulate expression and enzymatic activity of GTP cyclohydrolase, *i.e.* the rate-limiting enzyme in biosynthesis of H4B, in vascular endothelial cells (50). Beside enhancing the eNOS activity, H4B additionally enhances the enzymatic activity of iNOS (46). Thus, at elevated H4B concentrations formation of peroxynitrite might be stimulated because of an enhanced production of both nitric oxide from iNOS-bound H4B and $O_2^{\bullet -}$ from autoxidation of freely diffusing tetrahydrobiopterin. In fact, an increase in both vascular tetrahydrobiopterin production and iNOS activity was evident in aortas of apolipoprotein E-deficient mice (51). Furthermore, neopterin, a byproduct of H4B biosynthesis (46, 52) was found to be increased in plasma of patients with pulmonary tuberculosis, lung cancer (53), or atherosclerosis (54). There are very strong indications for the intermediacy of $O_2^{\bullet -}$/peroxynitrite in the latter illness (55–57). In contrast to an increasing number of papers, *e.g.* (18, 39, 41, 42, 46, 52), where H4B is suggested to be a target for harmful radicals (*e.g.* $O_2^{\bullet -}$), the data presented here provided sound evidence that non-protein-bound tetrahydrobiopterin generates and consumes $O_2^{\bullet -}$ and can therefore induce oxidative stress at elevated levels. This sheds new light on the elevation of endogenous tetrahydrobiopterin levels in atherosclerotic arteries (46).

Acknowledgment—The present investigation would have been impossible without the perfect technical assistance of A. Wensing.

REFERENCES

1. Kaufman, S. (1958) *J. Biol. Chem.* **230,** 931–939
2. Kwon, N. S., Nathan, C. F., and Stuehr, D. J. (1989) *J. Biol. Chem.* **264,** 20496–20501
3. Mayer, B., and Hemmens, B. (1997) *Trends Biochem. Sci.* **22,** 477–481
4. Tayeh, M. A., and Marletta, M. A. (1989) *J. Biol. Chem.* **264,** 19654–19658
5. Schmidt, H. H. H. W., Poolock, J. S., Förstermann, U., and Murad, F. (1991) *FASEB J.* **5,** A1591
6. Fisher, D. B., and Kaufman, S. (1973) *J. Biol. Chem.* **248,** 4300–4304
7. Blair, J. A., and Pearson, A. J. (1974) *J. Chem. Soc. Perkin II*, 80–88
8. Pearson, A. J. (1974) *Chem. Ind.* (*Lond.*) 233–238
9. Nishikimi, M. (1975) *Arch. Biochem. Biophys.* **166,** 273–279
10. Heikkila, R. E., and Cohen, G. (1975) *Experientia* **31,** 169–170
11. Kwee, S. (1987) *Bioelectrochem. Bioenerg.* **18,** 79–89
12. Hasegawa, H., Nakanishi, N., and Akino, M. (1978) *J. Biochem.* (*Tokyo*) **84,** 499–506
13. Liochev, S. I., and Fridovich, I. (1995) *Arch. Biochem. Biophys.* **318,** 408–410
14. Eberlein, G., Bruice, T. C., Lazarus, R. A., Henrie, R., and Benkovic, S. J. (1984) *J. Am. Chem. Soc.* **106,** 7916–7924
15. Davies, M. D., and Kaufman, S. (1993) *Arch. Biochem. Biophys.* **304,** 9–16
16. Mayer, B., Klatt, P., Werner, E. R., and Schmidt, K. (1995) *J. Biol. Chem.* **270,** 655–659
17. Xia, Y., and Zweier, J. L. (1997) *Proc. Natl. Acad. Sci. U. S. A.* **94,** 12705–12710
18. Vasquez-Vivar, J., Whitsett, J., Martasek, P., Hogg, N., and Kalyanaraman, B. (2001) *Free Radical Biol. Med.* **31,** 975–985
19. Koshimura, K., Murakami, Y., Tanaka, J., and Kato, Y. (1998) *J. Neurosci. Res.* **54,** 664–672
20. Shimizu, S., Ishii, M., Kawakami, Y., Momose, K., and Yamamoto, T. (1998) *Life Sci.* **63,** 1585–1592
21. Kirsch, M., Lomonosova, E. E., Korth, H.-G., Sustmann, R., and de Groot, H. (1998) *J. Biol. Chem.* **273,** 12716–12724
22. Davies, M. D., Kaufman, S., and Milstien, S. (1988) *Eur. J. Biochem.* **173,** 345–351
23. Meineke, P., Rauen, U., de Groot, H., Korth, H.-G., and Sustmann, R. (1999) *Chem. Eur. J.* **5,** 1738–1747
24. Meineke, P., Rauen, U., de Groot, H., Korth, H.-G., and Sustmann, R. (2000) *Biol. Chem.* **381,** 575–582
25. Ioannidis, I., and de Groot, H. (1993) *Biochem. J.* **296,** 341–345
26. Duling, D. R. (1994) *J. Magn. Reson. B* **104,** 105–110
27. Ramamurthi, A., and Lewis, R. S. (1997) *Chem. Res. Toxicol.* **10,** 408–413

28. von Sonntag, C., and Schuchmann, H. P. (1991) *Angew. Chem. Int. Ed. Engl.* **30,** 1229–1253
29. Armarego, W. L. F., Randles, D., and Taguchi, H. (1983) *Eur. J. Biochem.* **135,** 393–403
30. Pfeiffer, S., Gorren, A. C. F., Schmidt, K., Werner, E. R., Hansert, B., Bohle, D. S., and Mayer, B. (1997) *J. Biol. Chem.* **272,** 3465–3470
31. Keefer, L. K., Nims, R. W., Davies, K. M., and Wink, D. A. (1996) *Methods Enzymol.* **268,** 281–293
32. Kirsch, M., Korth, H.-G., Sustmann, R., and de Groot, H. (2000) *Chem. Res. Toxicol.* **13,** 451–461
33. Totter, J. R., de Dugros, E. C., and Riveiro, L. (1960) *J. Biol. Chem.* **235,** 1839–1842
34. Fridovich, I. (2001) *J. Biol. Chem.* **276,** 28629–28636
35. Vasquez-Vivar, J., Hogg, N., Pritchard, K. A., Martasek, P., and Kalyanaraman, B. (1997) *FEBS Lett.* **403,** 127–130
36. Liochev, S. I., and Fridovich, I. (1997) *Arch. Biochem. Biophys.* **337,** 115–120
37. Wardman, P., Burkitt, M. J., Patel, K. B., Lawrence, A., Jones, C. M., Everett, S. A., and Vojnovic, B. (2002) *J. Fluorescopy* **12,** 65–68
38. Vasquez-Vivar, J., Joseph, J., Karoui, H., Zhang, H., Miller, J., and Martasek, P. (2000) *Analusis* **28,** 487–492
39. Patel, K. B., Stratford, M. R. L., Wardman, P., and Everett, S. A. (2002) *Free Radical Biol. Med.* **32,** 203–211
40. Vasquez-Vivar, J., Kalyanaraman, B., Martasek, P., Hogg, N., Masters, B. S., Karoui, H., Tordo, P., and Pritchard, K. A., Jr. (1998) *Proc. Natl. Acad. Sci. U. S. A.* **95,** 9220–9225
41. Vasquez-Vivar, J., Hogg, N., Martasek, P., Karoui, H., Pritchard, K. A., and Kalyanaraman, B. (1999) *J. Biol. Chem.* **274,** 26736–27342
42. Rosen, G. M., Tsai, P., Weaver, J., Porasuphatana, S., Roman, L. J., Starkov, A. A., Fiskum, G., and Pou, S. (2002) *J. Biol. Chem.* **277,** 40275–40280
43. Misra, H. P., and Fridovich, I. (1972) *J. Biol. Chem.* **247,** 3170–3175
44. Heikkila, R. E., and Cohen, G. (1973) *Science* **181,** 456–457
45. Eberlein, G., and Bruice, T. C. (1983) *J. Am. Chem. Soc.* **105,** 6685–6697
46. Katusic, Z. S. (2001) *Am. J. Physiol.* **281,** H981–H986
47. Stroes, E., Kastelein, J., Cosentino, F., Erkelens, W., Wever, R., Koomans, H., Luscher, T., and Rabelink, T. (1997) *J. Clin. Invest.* **99,** 41–46
48. Maier, W., Cosentino, F., Lutolf, R. B., Fleisch, M., Seiler, C., Hess, O. M., Meier, B., and Luscher, T. F. (2000) *J. Cardiovasc. Pharmacol.* **35,** 173–178
49. Heitzer, T., Brockhoff, C., Mayer, B., Warnholtz, A., Mollnau, H., Henne, S., Meinertz, T., and Munzel, T. (2000) *Circ. Res.* **86,** E36–E41
50. Rosenkranz-Weiss, P., Sessa, W. C., Milstien, S., Kaufman, S., Watson, C. A., and Pober, J. S. (1994) *J. Clin. Invest.* **93,** 2236–2243
51. d′Uscio, L. V., Milstien, S., and Katusic, Z. S. (2002) *FASEB J.* **16,** A434
52. Walter, R., Schaffner, A., and Schoedon, G. (2001) *Pteridines* **12,** 93–120
53. Mohamed, K. H., Mobasher, A. A. M. T., Yousef, A.-R. I., Salah, A., El-Naggar, I. Z., Ghoneim, A. H. A., and Light, R. W. (2001) *CHEST* **119,** 776–780
54. Tatzber, F., Rabl, H., Koriska, K., Erhart, U., Puhl, H., Waeg, A., Krebs, A., and Esterbauer, H. (1991) *Atherosclerosis* **89,** 203–208
55. White, C. R., Brock, T. A., Chang, L. Y., Crapo, J., Briscoe, P., Ku, D., Bradley, W. A., Gianturco, S. H., Gore, J., Freeman, B. A., and Tarpey, M. M. (1994) *Proc. Natl. Acad. Sci. U. S. A.* **91,** 1044–1048
56. Brown, L. A. S., and Jones, D. P. (1996) in *Handbook of Antioxidants* (Cadenas, E., ed) Vol. 3, pp. 117–154, Marcel Dekker, New York
57. Beckman, J. S., Ye, Z. Y., Anderson, P. G., Chen, J., Accavitti, M. A., Tarpey, M. M., and White, C. R. (1994) *Biol. Chem. Hoppe-Seyler* **375,** 81–88
58. Bergmeyer, H. U., Grassl, M., and Walter, H.-E. (1983) in *Methods of Enzymatic Analysis* (Bergmeyer, H. U., ed) Vol. II, pp. 165, Verlag Chemie, Weinheim
59. Ross, A. B., Mallard, W. G., Helman, W. P., Buxton, G. V., Huie, R. E., and Neta, P. (1998) *NDRL/NIST Solution Kinetics Database 3.0*, NDRL/NIST, Gaithersburg, MD
60. Kirsch, M., Lehnig, M., Korth, H.-G., Sustmann, R., and de Groot, H. (2001) *Chem.-Eur. J.* **7,** 3313–3320
61. Eigen, M. (1964) *Angew. Chem. Int. Ed. Engl.* **3,** 1–19
62. Koppenol, W. H., Moreno, J. J., Pryor, W. A., Ischiropoulos, H., and Beckman, J. S. (1992) *Chem. Res. Toxicol.* **5,** 834–842
63. Coddington, J. W., Hurst, J. K., and Lymar, S. V. (1999) *J. Am. Chem. Soc.* **121,** 2438–2443
64. Goldstein, S., Saha, A., Lymar, S. V., and Czapski, G. (1998) *J. Am. Chem. Soc.* **120,** 5549–5554
65. Merenyi, G., Lind, J., Goldstein, S., and Czapski, G. (1999) *J. Phys. Chem. A* **103,** 5685–5691
66. Kirsch, M., Korth, H.-G., Sustmann, R., and de Groot, H. (2002) *Biol. Chem.* **383,** 389–399
67. Goldstein, S., Czapski, G., Lind, J., and Merenyi, G. (1998) *Inorg. Chem.* **37,** 3943–3947
68. Logager, T., and Sehested, K. (1993) *J. Phys. Chem.* **97,** 10047–10052
69. Goldstein, S., and Czapski, G. (1997) *Inorg. Chem.* **36,** 4156–4162
70. Goldstein, S., and Czapski, G. (1996) *J. Am. Chem. Soc.* **118,** 3419–3425
71. Schwartz, S. E., and White, W. H. (1981) *Adv. Environ. Sci. Technol.* **4,** 1
72. Markovits, G. Y., Schwartz, S. E., and Newman, L. (1981) *Inorg. Chem.* **20,** 445–450
73. Caccia, S., Denisov, I., and Perrella, M. (1999) *Biophys. Chem.* **76,** 63–72
74. Wolfe, S. K., and Swinehart, H. J. (1975) *Inorg. Chem.* **14,** 1049–1053